

Landslides on coastal sage-scrub and grassland hillslopes in a severe El Niño winter: The effects of vegetation conversion on sediment delivery

Emmanuel J. Gabet*

Department of Geological Sciences, University of California, Santa Barbara, California 93106, USA

Thomas Dunne

Donald Bren School of Environmental Science and Management and Department of Geological Sciences, University of California, Santa Barbara, Santa Barbara, California 93106, USA

ABSTRACT

During the 1997–1998 El Niño, record rainfall triggered >150 shallow landslides within a 9.5 km² area near Santa Barbara, California. They were studied to analyze the sediment delivery to valley floors from landslides in coastal sage scrub and converted grasslands. The conversion of coastal sage to grasslands, primarily to provide pasturage for cattle, is common in the region, and the landscape's response may affect water quality, reservoir infilling, and debris flow hazards. We explore the relationship between lateral-root reinforcement and landslide volume by developing a slope-stability analysis that incorporates root cohesion along the sides of the failure. The stability analysis correctly predicts an inverse relationship between landslide volume and hillslope angle in the sage. The volumes of failures in the grasslands do not vary systematically with slope and are generally smaller than those in the sage. From aerial-photograph analysis and field mapping, we find that there are 22.9 failures per square kilometer in the grasslands compared to 13.2 failures per square kilometer in the sage. Despite the lower failure density in the coastal sage, greater failure volumes and longer transport distances delivered more sediment to valley floors, with a specific volumetric flux of $2.8 \times 10^{-2} \text{ m}^3\text{m}^{-1}$ for this El Niño compared to $1.7 \times 10^{-2} \text{ m}^3\text{m}^{-1}$ in the grasslands. We conclude that the conversion from vegetation with stronger and deeper roots (coastal sage) to vegetation with weaker and shallower roots (grass) has caused a pulse of increased landsliding in the grasslands because the soils are currently too thick for the prevailing root reinforcement. We suggest that, over time, soils in the grassland hollows will become thinner as the evacuation by landslides is repeated until the landsliding rate declines to balance the soil supplied from local colluvium production and diffusive processes upslope.

Keywords: debris flows, geomorphology, landslides, sediment supply, sediment transport, slope stability.

*E-mail: egabet@bren.ucsb.edu.

INTRODUCTION

The El Niño event of 1997–1998 struck the coast of Santa Barbara County, California, with exceptional ferocity, producing the single wettest month and the second wettest year that the region has experienced in more than 100 yr. On the night of February 3–4, 1998, after several days of heavy rainfall (Fig. 1), more than 150 shallow landslides were triggered in a 9.5 km² area at Sedgwick Ranch, 60 km north of Santa Barbara. Although Sedgwick Ranch has a range of vegetation communities, including pine forest, the landslides were limited to hillslopes vegetated by coastal sage scrub (Fig. 2A) or exotic grasses (Fig. 2B). Whereas all the failures in the sage mobilized as debris flows, the failures in the grass took a variety of different forms, including debris flows, disintegrating soil slips (Kesseli, 1943), and slumps (*sensu* Kesseli, 1943).

Shallow landslides, or *soil slips* (Kesseli, 1943; Corbett and Rice, 1966), are characterized by a failure surface at the soil-bedrock contact and typically occur in bedrock hollows, which are unchannelized swales on hillslopes (e.g., Reneau et al., 1990). Hollows accumulate sediment transported from adjacent slopes for hundreds to thousands of years (e.g., Campbell, 1975; Reneau et al., 1990), and as the soil in a hollow thickens over time, it becomes increasingly prone to failure during heavy rainfall (Rice et al., 1969). After failure, the hollow begins filling up again, and the cycle repeats itself (Dietrich and Dunne, 1978). Land-management strategies may amplify the susceptibility of hillslopes to landsliding. In the Pacific Northwest, for example, increased shallow landsliding has been attributed to logging that has decreased the contribution of tree roots to slope stability (Montgomery et al., 2000). In drier regions of the American West, hillslopes are cleared of brush and converted to grasslands primarily to increase forage for livestock (Rice and Foggin, 1971) and, secondarily, to reduce fire hazards and increase water yields (Hibbert, 1971). As in the logged forests, this management strategy has decreased soil reinforcement by roots (Terwilliger and Waldron, 1991) and increased landsliding in converted areas of southern California (Corbett and Rice, 1966; Bailey and Rice, 1969; Rice et al., 1969; Rice and Foggin, 1971).

Understanding the effect of vegetation conversion on landslide frequency in southern California and similar areas is critical because studies by Rice and Foggin (1971) and Scott (1971) suggest that shallow

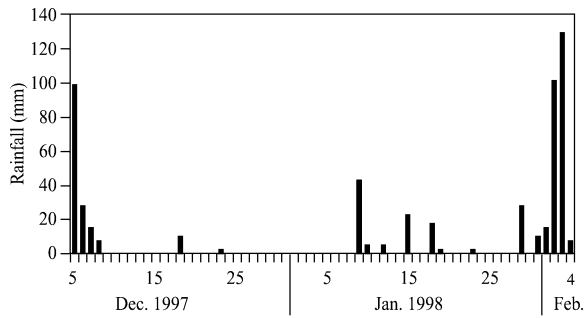


Figure 1. Daily rainfall totals from Figueroa Mountain Ranger Station (elev. 976 m), 3 km northeast of Sedgwick Ranch (elev. 480 m). The difference in elevations suggests that the totals would have been less at Sedgwick Ranch. The landsliding occurred on the night between February 3 and 4, 1998. Data provided by NOAA (National Oceanic and Atmospheric Administration).

landslides may be responsible for the majority of sediment issuing from small watersheds. Increased rates of sediment delivery from hillslopes may affect a number of important concerns such as water quality and the infilling of reservoirs constructed for water storage and flood control (Lustig, 1965; Rice and Foggin, 1971). Additionally, the proliferation of housing developments on alluvial fans exacerbates the danger from debris flows (Campbell, 1975) and flooding (Scott, 1971), which are both linked to landsliding (Rice and Foggin, 1971). Finally, examining the effects of human-induced vegetation change on sediment production may provide insights into the effects of climatically driven vegetation change.

We studied the landslides triggered by the 1997–1998 El Niño to gain a better understanding of shallow landsliding in this environment and the role of vegetation conversion in affecting the rates and mechanics of this process. We are motivated by three questions. First, how does root reinforcement influence the volume of a failure? Second, how do the landscape-scale sediment fluxes to valley floors compare between hillslopes covered by sage and those converted to grass? Third, what are some of the long-term geomorphic consequences of vegetation conversion to hillslope processes?

FIELD SITE

Sedgwick Ranch, a reserve in the University of California Natural Reserve System, is located on the northern margin of the Santa Ynez Valley, in the western Transverse Ranges. The ranch is bisected by the Little Pine fault, which separates Pleistocene fanglomerates of the Paso Robles Formation on one side from serpentinites and graywackes of the Franciscan Formation on the other (Dibblee, 1993). The landslides triggered in 1998 occurred where the Paso Robles Formation has been incised by small streams to produce gentle to moderately steep, rolling hillslopes with an average relief of 60–100 m. Hillslope gradients are controlled by the bedrock; weakly consolidated mudstone underlies most of this area and supports slopes up to 32°. Steeper hillslopes (32°–45°) are supported by interbeds of cemented conglomerate. Soil textures range from sandy loams to silty clays.

The semiarid Mediterranean climate averages 50 cm of annual rainfall. Many hillslopes at Sedgwick Ranch are currently vegetated by exotic, annual grasses (various species of *Bromus* and *Avena*), although grass is not found on slopes steeper than 35° where coastal sage scrub still dominates (mainly *Artemisia californica* and *Salvia leucophylla*). The spatial distribution of the two vegetation types is distinct; only a narrow range of overlap (<10 m) exists where they abut. The history of vegetation conversion at Sedgwick Ranch is not known, but the earliest aerial photographs indicate that the present distribution of vegetation was established before the 1930s. Hamilton (1997) proposed that most nonnative grasslands in the region were formerly dominated by coastal sage scrub, and there is substantial evidence indicating that sage was the original vegetation on the grassland slopes at Sedgwick Ranch. On some hillslopes, the boundary between the grasslands and the sage is sharp, and they grow side by side, separated only by a fence. Additionally, in many cases, grass grows on the lower part of the slopes where gradients are more gentle, whereas the steeper, upper parts are dominated by sage. This distribution suggests that the gentler slopes were manually cleared, whereas the steeper ones were left undisturbed (Campbell, 1975). Finally, remnants of roots with diameters of 5–10 mm have been found in soil pits excavated on the grass slopes, an indication that these slopes were once covered by shrubs rather than native bunch grasses. Clearing slopes of coastal sage mechanically or by prescribed burn continues to be a common practice in the region.

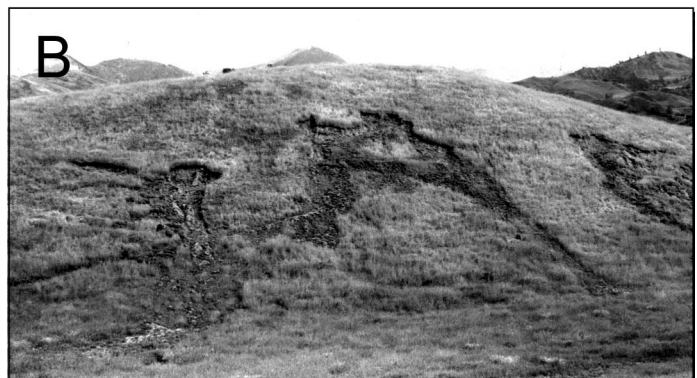
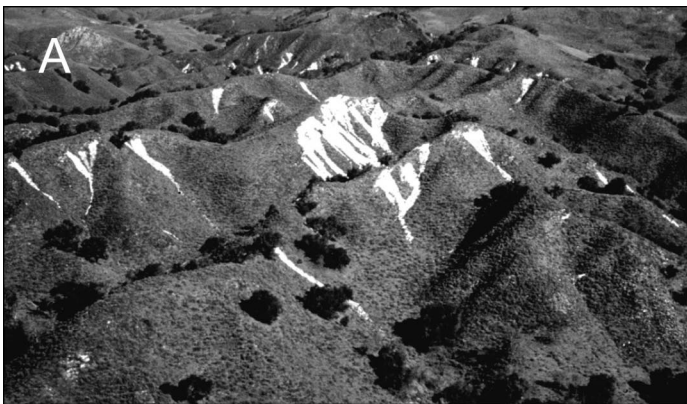


Figure 2. (A) Shallow landslides (white areas) in the sage. Note that the failures originated in hillslope concavities (hollows). (B) Landslides in the converted grasslands triggered on flat and convex parts of the hillslope.

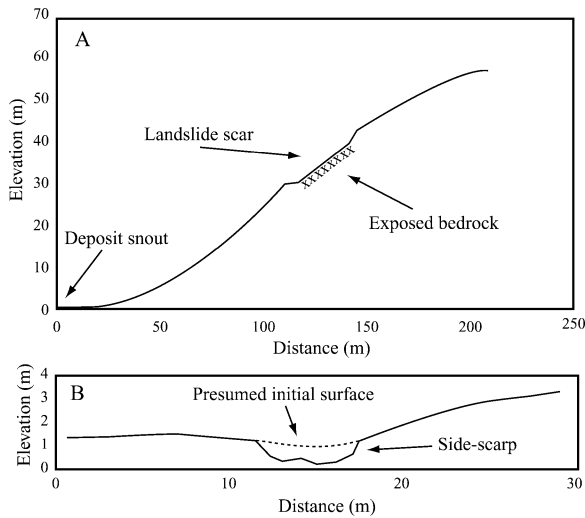


Figure 3. (A) Longitudinal profile of hillslope with landslide scar. (B) Cross section of scar shown in longitudinal profile. The initial surface was reconstructed from the adjacent topography. (Both figures have 2× vertical exaggeration.)

METHODS

Mapping

Two months after the landsliding occurred, stereo color aerial photographs at 1:21 000 scale were taken of the field site. These were used to identify and map the landslides onto the U.S. Geological Survey Los Olivos 7.5' topographic map. Smaller slides that were difficult to see on the photographs were mapped in the field.

A vegetation map was created from the aerial photographs to determine the area covered by each vegetation type. Because we were specifically interested in landsliding, only hillslopes steeper than 15°, the lowest slope observed with a failure, were included in the area calculations.

Surveying

A subset of 31 landslides was randomly chosen to sample the range of failure sizes and hillslope gradients. These were surveyed with a tape, stadia rod, and level. A longitudinal profile of each failure was surveyed from the hillslope divide, down the failure scar, to the snout of the deposit (Fig. 3A). During the longitudinal survey, the location of the center of mass of each deposit was visually estimated to determine transport distance. Three to five cross sections were surveyed across each failure, and the initial surface was reconstructed from the surrounding topography (Fig. 3B) to estimate volumes of sediment evacuated. Data from these surveys are presented in Table 1.

A Tesco variably loaded shear vane was used to measure, in situ, the internal angle of friction and cohesion of soils at the landslide sites. The blades of the vane only penetrate to a depth of 0.5 cm so that the effect of roots on the measurements is minimized.

LANDSLIDE VOLUMES

The volume of individual failures is an important factor in sediment delivery, and the debris flows in the sage were generally larger than

TABLE 1. LANDSLIDES CHARACTERISTICS

| Site | Scar angle (°) | Area (m ²) | Volume (m ³) | Depth (m) | Width (m) | Length (m) | Length Width | Run-out distance (m) | Snout angle (°) | C.O.M. distance* (m) |
|--|----------------|------------------------|--------------------------|-----------|-----------|------------|--------------|----------------------|-----------------|----------------------|
| Slumps on grass slopes | | | | | | | | | | |
| 1 | 31 | 26 | | | 4.8 | 6.6 | 0.7 | | | |
| 2 | 29 | 26 | | | 5.9 | 5.2 | 1.1 | | | |
| 3 | 27 | 63 | | | 7.6 | 8.0 | 1.0 | | | |
| 4 | 23 | 99 | | | 10.0 | 10.1 | 1.0 | | | |
| 5 | 17 | 142 | | | 13.4 | 11.0 | 1.2 | | | |
| 6 | 26 | 142 | | | 11.0 | 12.9 | 0.9 | | | |
| Avg | 26 | 83 | | | 9 | 8.8 | 1.1 | | | |
| 1σ | 5 | 53 | | | 2.9 | 3.3 | 0.2 | | | |
| Disintegrating soil slips on grass slopes | | | | | | | | | | |
| 1 | 23 | 204 | 62 | 0.30 | 11.0 | 41.0 | 3.7 | 36 | 25 | 30 |
| 2 | 23 | 154 | 40 | 0.26 | 6.9 | 26.1 | 3.8 | 56 | 22 | 63 |
| 3 | 23 | 389 | 131 | 0.34 | 14.0 | 39.7 | 2.8 | 196 | 5 | 190 |
| Avg | 23 | 249 | 78 | 0.30 | 10.6 | 35.6 | 3.4 | 96 | 17 | 94 |
| 1σ | 0 | 123 | 48 | 0.04 | 3.6 | 8.3 | 0.6 | 87 | 11 | 85 |
| Debris flows on grass slopes | | | | | | | | | | |
| 1 | 29 | 114 | 84 | 0.74 | 5.4 | 25.6 | 4.7 | 36 | 20 | 22 |
| 4 | 29 | 32 | 11 | 0.34 | 2.8 | 12.7 | 4.5 | 27 | 6 | 13 |
| 6 | 30 | 64 | 33 | 0.52 | 6.9 | 9.4 | 1.4 | 130 | 3 | 95 |
| 9 | 30 | 92 | 50 | 0.54 | 6.1 | 14.4 | 2.4 | 66 | 8 | 54 |
| 15 | 25 | 65 | 28 | 0.43 | 6.1 | 10.7 | 1.8 | 48 | 20 | 12 |
| 19 | 27 | 52 | 23 | 0.44 | 4.6 | 12.5 | 2.7 | C | C | C |
| 20 | 32 | 15 | 6 | 0.37 | 3.4 | 4.4 | 1.3 | C | C | C |
| Avg | 29 | 62 | 33 | 0.48 | 5.0 | 12.8 | 2.7 | 61 | 11 | 39 |
| 1σ | 2 | 34 | 27 | 0.13 | 1.5 | 6.5 | 1.4 | 41 | 8 | 35 |
| Debris flows on sage slopes | | | | | | | | | | |
| 3 | 32 | 257 | 160 | 0.62 | 12.2 | 20.7 | 1.7 | 132 | 7 | 27.4 |
| 5 | 32 | 173 | 89 | 0.51 | 17.0 | 11.6 | 0.7 | 74 | 7 | 26.1 |
| 7 | 43 | 35 | 13 | 0.37 | 3.2 | 10.8 | 3.4 | 26 | 18 | 20.4 |
| 8 | 34 | 110 | 70 | 0.64 | 7.3 | 15.1 | 2.1 | C | C | C |
| 10 | 32 | 216 | 114 | 0.53 | 8.8 | 24.7 | 2.8 | 63 | 10 | 43.5 |
| 11 | 35 | 103 | 72 | 0.70 | 8.8 | 12.5 | 1.4 | C | C | C |
| 12 | 35 | 145 | 75 | 0.52 | 7.2 | 22.0 | 3.1 | C | C | C |
| 13 | 37 | 117 | 52 | 0.44 | 8.3 | 14.6 | 1.8 | C | C | C |
| 14 | 35 | 108 | 46 | 0.43 | 4.4 | 24.8 | 5.6 | C | C | C |
| 16 | 35 | 206 | 145 | 0.70 | 8.2 | 25.3 | 3.1 | 86 | 20 | 42.8 |
| 17 | 45 | 41 | 11 | 0.27 | 3.0 | 13.7 | 4.6 | 7 | 30 | 10.1 |
| 23 | 39 | 111 | 45 | 0.41 | 6.2 | 22.3 | 3.6 | 73 | 3 | 55.5 |
| 24 | 39 | 96 | 44 | 0.46 | 5.8 | 15.8 | 2.7 | C | C | C |
| 25 | 40 | 248 | 91 | 0.37 | 9.2 | 27.1 | 3.0 | C | C | C |
| 26 | 34 | 106 | 64 | 0.60 | 7.7 | 13.3 | 1.7 | 39 | 0 | 27.7 |
| Avg | 37 | 138 | 73 | 0.5 | 7.1 | 18.3 | 2.7 | 54 | 13 | 36 |
| 1σ | 4 | 68 | 43 | 0.13 | 3.5 | 5.7 | 1.2 | 31 | 12 | 18 |

Note: Avg—average, 1σ—1 standard deviation. The scars of the disintegrating soil slips appeared to have been the result of several failures coalescing. Depth, width, and length data are averages for each failure. Snout angle refers to the slope at which the snout was deposited. C indicates that a portion of the deposit was removed by channelized flow, and, therefore, the distance measurements could not be made. Soil depth, volume, and run-out distance are not given for slumps because they did not evacuate the scar.

*C.O.M. distance is the distance from the middle of the scar to the center of mass of the deposit.

those in the grass (Table 1). Although the size of the disintegrating soil slips in the grass was approximately equal to that of the debris flows in the sage, the disintegrating soil slips appeared to have been composed of several smaller failures. On the sage-covered slopes, a physical relationship between failure volume and hillslope angle is suggested by the inverse relationship between the two (Table 1) and is revealed by an examination of the various forces on a failing soil mass. The commonly used infinite-slope stability analysis for shallow landslides (Selby, 1993) can predict soil depths at failure (Dietrich et al., 1995), but because it assumes that the failing mass is infinitely long and wide, it cannot be used to determine failure length and width. This stability analysis only considers root cohesion in the vertical direction, and it is usually applied in forested regions where cohesive reinforcement occurs along the basal surface (e.g., Sidle, 1987). In environments where roots do not penetrate bedrock and fail to anchor the soil ver-

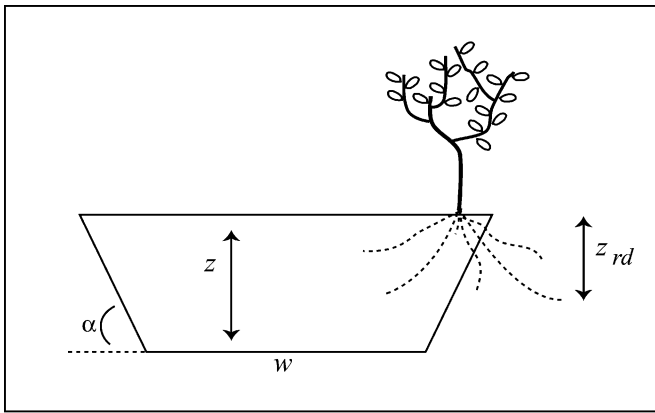


Figure 4. Illustration of the geometrical relationships pertaining to the cohesion terms in the stability analysis (compare with the cross section in Fig. 3B). Soil cohesion is applied to the perimeter of the failure: $W + 2z \cos \theta / \sin \alpha$. Root cohesion only acts over the perimeter to the extent of the rooting depth: $2z_{rd} \cos \theta / \sin \alpha$.

tically, root reinforcement is solely in the lateral direction. This distinction is critical because accounting for the lateral reinforcement of roots in a stability analysis requires modification of the infinite-slope model. The infinite-slope model only considers stresses and strengths on the basal slip surface, so it should not be used when lateral-root reinforcement is important.

Others have adapted the infinite-slope model to account for lateral-root contributions, and this approach has allowed for the examination of the relationship between failure dimensions and root cohesion. Reineau and Dietrich (1987) investigated the link between lateral-root cohesion and failure size by modifying the stability analysis derived by Reistenberg and Sovonick-Dunford (1983). However, their approach does not produce unique solutions for landslide dimensions. Terwilliger and Waldron (1991) presented a three-dimensional analysis to study the effects of root-cohesion distributions on failure size. Their analysis considers many important details of slope stability, such as the mechanical behavior of roots during the initial moments of failure.

In contrast to Terwilliger and Waldron (1991), we derive a simpler analysis with fewer data requirements to examine the relationship between hillslope angle and failure volume at Sedgwick Ranch. Instead of the infinite-slope model, which assumes that the forces on the sides of the failure are negligible, we present a force balance that considers the forces on a slice of hillslope taken parallel to the contour lines and that accounts for reinforcement along the side scarps of the failures (Fig. 4). To include the forces along the edges of the failure mass, the stability analysis presented here is derived so that the terms represent forces per unit length of slope, rather than forces per unit area of slope. We assume, therefore, a landslide that is infinitely long but with a finite width.

Shallow-landslide stability analyses are typically idealized as a block on an inclined plane (e.g., Selby, 1993), and the ratio of the resisting forces to the disturbing forces defines the factor of safety (f) so that the block is stable when $f > 1$. The forces per unit length can be resolved by assuming that the block is sufficiently long relative to the width so that the difference between the forces on the uphill and downhill ends of the block is negligible (e.g., Selby, 1993). The disturbing force is the downslope component of the weight of the block:

$$\frac{F_s}{l} = wz\gamma_s \cos \theta \sin \theta, \quad (1)$$

where

- F_s = shear force (kN)
- l = failure length (m)
- w = failure width (m)
- z = soil depth measured vertically (m)
- γ_s = unit weight of wet soil (kN m^{-3})
- θ = hillslope angle ($^\circ$)

The resisting force includes the effective normal component of the weight of the block mediated by the internal angle of friction (ϕ) (Selby, 1993),

$$\frac{F_f}{l} = wz(\gamma_s - m\gamma_w) \cos^2 \theta \tan \phi, \quad (2)$$

where

- F_f = frictional resistance (kN)
- m = fraction of the soil column that is saturated
- γ_w = unit weight of water (kN m^{-3}).

In addition to friction, soil strength is provided by soil cohesion and lateral-root reinforcement. Soil cohesion acts over the entire perimeter of the failure surface, whereas root reinforcement acts over the perimeter only to the extent of the rooting depth (Fig. 4) so that

$$R_s = C_s \left(w + \frac{2z \cos \theta}{\sin \alpha} \right) \quad \text{and} \quad (3a)$$

$$R_r = C_{rl} \left(\frac{2z_{rd} \cos \theta}{\sin \alpha} \right), \quad (3b)$$

where

- C_{rl} = lateral root cohesion (kPa)
- C_s = soil cohesion (kPa)
- R_r = total reinforcement by roots (kN m^{-1})
- R_s = total reinforcement from soil cohesion (kN m^{-1})
- z_{rd} = rooting depth measured vertically (m)
- α = angle of side-scarp ($^\circ$).

Lateral earth forces were calculated (Craig, 1978) and found to account for only 10% of the total resistance, so we consider them negligible given the uncertainty in the other terms. The resisting force is the sum of the frictional and cohesive forces (e.g., Craig, 1978), so the factor of safety is then

$$f = \frac{C_s \left(w + \frac{2z \cos \theta}{\sin \alpha} \right) + C_{rl} \left(\frac{2z_{rd} \cos \theta}{\sin \alpha} \right) + wz(\gamma_s - m\gamma_w) \cos^2 \theta \tan \phi}{wz\gamma_s \cos \theta \sin \theta}. \quad (4)$$

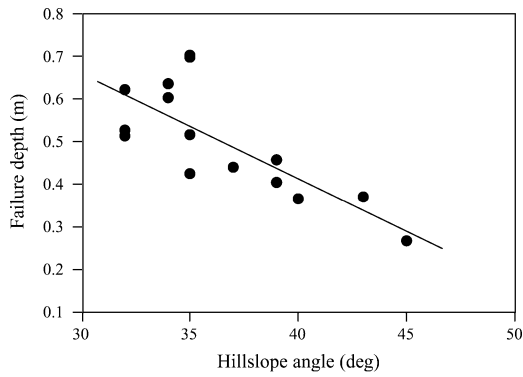


Figure 5. Average failure depth (z) vs. hillslope angle (θ). The line is the least-squares linear regression ($r^2 = 0.58$).

Again, because roots did not penetrate bedrock in any of the surveyed landslides at Sedgwick Ranch, we have not included a vertical root-anchoring term. Equation 4 can be solved for the failure width (i.e., $f = 1$) at different slope angles,

$$w = \frac{C_s \left(\frac{2z \cos \theta}{\sin \alpha} \right) + C_{ri} \left(\frac{2z_{rd} \cos \theta}{\sin \alpha} \right)}{z \cos \theta [\gamma_s \sin \theta - (\gamma_s - m\gamma_w) \cos \theta \tan \phi] - C_s}. \quad (5)$$

To demonstrate the dependence of failure width on hillslope angle and to compare the results to the field data, equation 5 is parameterized to reflect the average conditions on sage-covered slopes at Sedgwick Ranch. An average failure depth for each landslide was determined by dividing the failure volume by the planform area. For failures in the sage, Figure 5 shows a monotonic decline in average failure depth with slope ($r^2 = 0.58$, $n = 15$, $p < 0.005$),

$$z = 1.41 - 0.025\theta, \quad (6)$$

so that z in equation 5 can be calculated as a function of slope angle.

We set the rooting depth (z_{rd}) equal to the soil depth (z) at all gradients because, although we have observed long roots in the sage (>1 m), they were unable to penetrate the bedrock and were limited to growing along the soil-bedrock contact. Terwilliger and Waldron (1990) measured the root-cohesion contributions of chaparral and grass with direct shear tests and determined a root cohesion value of 3 kPa for chaparral. The soils that Terwilliger and Waldron (1990) sampled were primarily vegetated by chamise (*Adenostoma fasciculatum*), which grows taller than the coastal sage vegetation studied here. However, chamise roots are relatively thin (Hellmers et al., 1955), suggesting that using the root-cohesion values measured by Terwilliger and Waldron (1990) in the chamise may be appropriate for the sage.

There are two other important caveats to our root-cohesion representation. First, we assume that root cohesion does not change with depth, whereas Hellmers et al. (1955) noted that the highest concentrations of sage roots are near the soil surface. However, given the uncertainty in the root-cohesion values, we consider a uniform vertical root-cohesion distribution to be adequate, and this assumption is supported by data from Terwilliger and Waldron (1991). Second, the lateral distribution of root cohesion is also assumed to be uniform. Whereas Terwilliger and Waldron (1991) explicitly represented the lateral heterogeneity of chaparral root cohesion in their stability analysis,

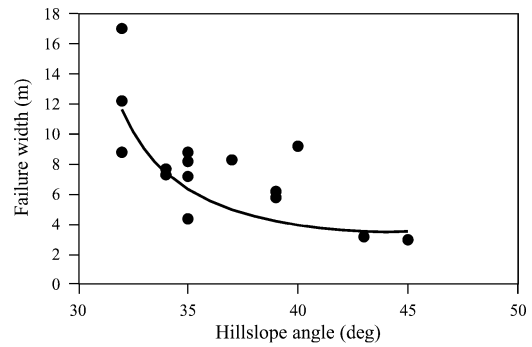


Figure 6. Comparison of predicted failure widths (line) and surveyed widths (points) as a function of hillslope angle for shallow landslides in the sage ($r^2 = 0.37$). Predicted widths were determined with Equation 5 and suggest that root cohesion exerts a dominant control on failure widths when lateral-root reinforcement is significant.

the dense cover of coastal sage scrub at Sedgwick Ranch suggests that the assumption of a laterally homogeneous root-cohesion distribution may be suitable.

Average values from Sedgwick Ranch for the side scarp angle and the unit weight of wet soil are 45° and $17.7 \text{ kN}\cdot\text{m}^{-3}$, respectively, and the unit weight of water is $9.81 \text{ kN}\cdot\text{m}^{-3}$. The angle of internal friction, 32° , is an average determined from 10 sites measured in situ at Sedgwick Ranch with a variably loaded shear vane. Unfortunately, the soil-cohesion values measured with the shear vane are unreliable because of the sensitivity of soil cohesion to water content (Selby, 1993). Ideally, these tests would be done on saturated soils to replicate the conditions at failure; however, they were done when the soils were damp. Consequently, there are no measured constraints on the parameter C_s . We are also unable to set constraints on m , a hydrological variable that depends on rainfall amounts and site-specific topography. These two variables, therefore, are used to fit equation 5 to the data. Thus, rather than trying to accurately reproduce the conditions at failure with incomplete data, we seek to explain the observed trend in failure volumes.

Various combinations of realistic values for C_s and m provide reasonable matches between equation 5 and the surveyed failure widths. In Figure 6, the field data for the failures in the sage are compared to the predicted failure widths with values of 0.7 kPa and 0.5 for C_s and m , respectively. Alternatively, the decrease in failure widths with increasing slope might also be explained otherwise. Bedrock hollows are generally narrower on steep slopes, and the width of the hollow sets an upper limit on the width of the failure contained within it. Of course, the width of the hollows themselves may be a long-term consequence of narrower failures on steeper slopes.

Landslide volumes on the sage-covered hillslopes can be calculated as a function of slope as the product of the widths predicted in Figure 6, the lengths determined from the average length/width ratio (2.7; Table 1), and the slope-dependent soil depths (equation 6). Figure 7 demonstrates that the stability analysis derived here may be used in conjunction with field data to predict landslide volumes. This finding may have important applications and could be integrated into topographically based models for shallow-landslide hazards (e.g., Dietrich et al., 1995), wherever the soil-depth function and the length/width relationships are defined from local data. Finally, the steep increase in failure widths as slopes become more gentle (Fig. 6) suggests that there

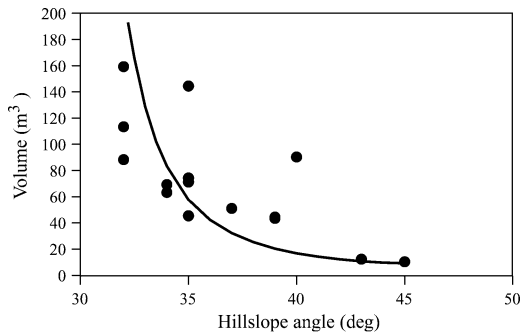


Figure 7. Comparison of predicted volumes (line) and surveyed volumes (points) as a function of hillslope angle for shallow landslides in the sage. Predicted volumes are calculated as the product of the slope-dependent soil depths (equation 6), the widths predicted in Figure 6, and the lengths determined from the average length/width ratio (Table 1). The predicted volumes are similar to the surveyed volumes ($r^2 = 0.46$; $r^2 = 0.53$ without the outlier at 40°).

TABLE 2. PARAMETER VALUES

| | |
|--------------------|------------|
| C_{ri} (grass)* | 1 kPa |
| C_s | 0.7 kPa |
| w^{\dagger} | 5 m |
| z^{\dagger} | 0.48 m |
| z_{sd}^{\dagger} | 0.15 m |
| α^{\dagger} | 45° |
| ϕ^{\dagger} | 32° |

*Terwilliger and Waldron (1991).

[†]Average value from field data.

is a minimum angle at which slopes will fail in the sage-covered areas; indeed, there were no observed failures in the sage at slopes of $<32^\circ$.

On the grass-covered hillslopes, there is no apparent trend in the volumes of failures with slope (Table 1), possibly owing to the relatively weaker contribution of grass roots to the total soil strength. This relationship can be appreciated analytically if

$$R_s \gg R_r \tag{7a}$$

and

$$w \gg z. \tag{7b}$$

With the data presented in Table 2, values for the reinforcement from soil cohesion (R_s) and apparent root cohesion (R_r) are $4.3 \text{ kN}\cdot\text{m}^{-1}$ and $0.4 \text{ kN}\cdot\text{m}^{-1}$, respectively; furthermore, failure widths (w) are generally an order of magnitude greater than failure depths (z ; Table 1). With the conditions in equations 7a and 7b satisfied for grassland failures, equation 4 then becomes the familiar infinite-slope stability analysis (e.g., Selby, 1993),

$$f = \frac{C_s + z(\gamma_s - m\gamma_w)\cos^2\theta \tan \phi}{z\gamma_s \cos \theta \sin \theta}, \tag{8}$$

The width variable in equation 4 cancels out in equation 8, implying that the forces involved are no longer width dependent. For this reason, the widths of the failures on the grass slopes may be determined by factors not represented in a simple force balance.

Because the grasslands at Sedgwick Ranch are on gentler slopes, it is difficult to separate the effects of slope and vegetation on landslide volume; nonetheless, the data suggest that failures in the grasslands are smaller than those in the sage. Additionally, Rice and Foggin (1971) found that failures in converted grasslands are typically smaller than those in the brush for similar slope angles. However, this observation may not be always true; for example, Rice et al. (1969) reported larger landslides on grasslands than on brush-covered slopes.

SEDIMENT TRANSPORT

Debris-Flow Deposits

With landslide volume, the distance traveled by the failed soil mass is also an important variable in determining the magnitude of the sediment flux. Many of the lower-order valleys at Sedgwick Ranch are unchanneled, so the deposits of 13 of the 22 debris flows are intact, thus allowing measurement of transport distances. Most deposits were clearly defined and had lobate snouts 0.1–0.5 m high. In many cases, there was evidence that some fine-grained material continued farther, probably as the mass drained, but this material represents $<1\%$ of the whole failure. The runout distances of the deposits (Table 1) reflect the strong control that hillslope length has on transport distance. Most failures stopped when the snout reached the valley floor, with the tail of the deposit sometimes resting at steeper slopes. This configuration suggests that once the snout stopped, the rest of the mass was unable to flow around it and subsequently drained, solidifying in place. The center of mass of the deposit was generally located about two-thirds of the way along the total runout distance, indicating that the sediment was distributed along the length of the runout.

The snouts of the majority of the deposits stopped on slopes at or $<10^\circ$ (Table 1), similar to values compiled by Whipple (1994). The sage-scrub vegetation, however, arrested the soil mass of the smaller failures on relatively steep slopes (Table 1). On the grass slopes, the degree of liquefaction rather than the landslide volume seemed to have determined the depositional slope. The more fluidized failures stopped on the gentler slopes, whereas the more block-like failures stopped on steeper slopes.

Sediment Flux

The specific volumetric flux (q_s) is the rate at which a volume of soil is transported across a unit contour width of hillslope. In the following analysis, we only consider the failures with significant amounts of displacement—i.e., the disintegrating soil slips and the debris flows—and will hereafter refer to them as “mobilized failures.” Also, because we are interested in sediment transport by landsliding, we do not consider fluvial transport of landslide sediment that reached the channels. By using the average center of mass transport distances (\bar{d} ; Table 1), the average volumes (\bar{V} ; Table 1), and a failure density (adjusted to include only the mobilized failures for the grass-covered slopes), a landscape-scale sediment flux for this El Niño event can be calculated with

$$q_s = \bar{d} \times \bar{V} \times f_{\text{failure}} \tag{9}$$

There are 2.92 km^2 of grass-covered hillslopes and 6.53 km^2 of sage-covered hillslopes at Sedgwick Ranch. There were a total of 67 failures in the grass and 86 in the sage, producing a failure density of 22.9 failures per square kilometer in the grassland and 13.2 failures per

square kilometer in the sage. Whereas all the sage failures converted to debris flows, debris flows accounted for only 56% of the grass failures; disintegrating soil slips and slumps accounted for 22% each. These data yield a flux of $1.7 \times 10^{-2} \text{ m}^3 \cdot \text{m}^{-1}$ per event for the grass slopes and $2.8 \times 10^{-2} \text{ m}^3 \cdot \text{m}^{-1}$ per event for the sage slopes. Long-term sediment fluxes cannot be estimated because the recurrence interval of events of this magnitude is not known for the region, but there is no indication of a widespread occurrence of shallow failures in aerial photographs of the area dating back to the 1930s. However, because the sage and grass grow back rapidly, evidence for recent widespread landsliding may be undetectable.

In contrast to the results found here, Rice et al. (1969) and Rice and Foggin (1971) concluded that landsliding in converted grasslands produced more sediment than landsliding in the native shrub vegetation. These studies (Rice et al., 1969; Rice and Foggin, 1971), however, compared sediment production from hillslopes of similar gradients with different vegetation covers, whereas our data are somewhat confounded by the unequal distribution of vegetation types across the range of hillslope gradients.

Despite the much higher failure density on the grass slopes at Sedgwick Ranch, the total sediment flux from these slides was less than those on the sage-covered slopes. Although the failures in the grass occurred on gentler slopes, other factors that influence both the size of the failures and the transport distance limited their sediment delivery to the valley floors. Terwilliger and Waldron (1991) suggested that spatially homogeneous root-cohesion distributions may explain smaller failures in grasslands. Additionally, weaker grass roots will allow a soil mass to fail with a lower degree of saturation, thereby reducing the potential for liquefaction and the transport of soil significant distances.

LONG-TERM EFFECTS OF VEGETATION CONVERSION

The replacement of the native sage by exotic grasses appears to have caused a pulse of landsliding on converted hillslopes at Sedgwick Ranch. Similar observations have been made by others in southern California (Corbett and Rice, 1966; Bailey and Rice, 1969; Rice et al., 1969; Rice and Foggin, 1971; Terwilliger and Waldron, 1991). Terwilliger and Waldron (1991) suggested that spatial differences in root-cohesion distributions between chaparral and grass may be responsible for a greater occurrence of landsliding on recently converted grassland slopes. Although this suggestion may be correct, we prefer a more fundamental explanation, initially mentioned by Rice and Foggin (1971). In general, slope stability depends on a balance between root reinforcement and soil depth, so that stronger roots allow soils to become deeper before they fail. Over time, maximum soil depths in bed-rock hollows will come into equilibrium with the prevailing root reinforcement. If the hillslopes have a permanent drop in root reinforcement, then the soils will be too thick for the new root conditions, and landsliding should increase. To demonstrate this effect, stable soil depths under sage or grass cover were calculated as a function of hillslope angle by means of equation 4. We parameterized equation 4 with the same values as for Figure 6 with one exception: The failure width was set at 5 m for all slope angles to facilitate the comparison of stable soil depths for a range of slope angles for both vegetation types. The values for the grass-root parameters, C_{ri} and z_{rd} , are shown in Table 2. Figure 8 demonstrates that there is a range of soil depths that are stable under sage but unstable under grass. The lowering of root reinforcement by vegetation conversion, therefore, may render a larger part of the landscape vulnerable to landsliding. The importance of root reinforcement in slope stability is further emphasized by the

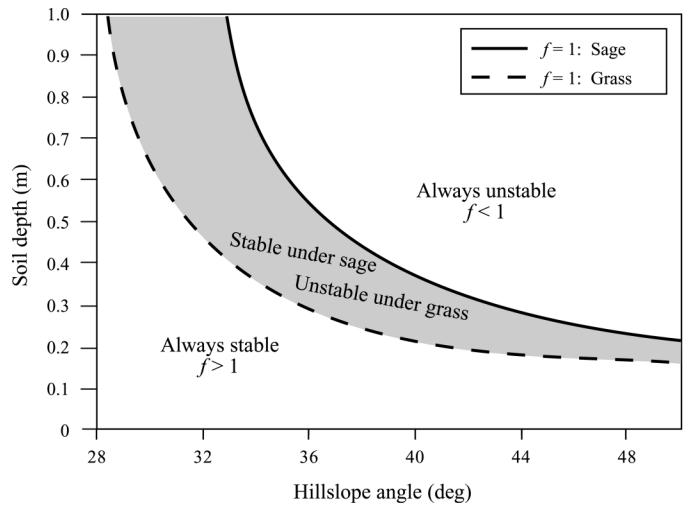


Figure 8. Stability analysis results for varying soil depths under sage or grass at different hillslope angles. The shaded area represents soil depths that are stable under sage but unstable under grass for identical soil-cohesion values and hydrological conditions. The “stability” line for the sage converges on the grass “stability” line because the root reinforcement in the sage is limited by the soil depth (i.e., $z_{rd} = z$). Failure depths do not decrease linearly with slope angle as in Figure 5 because failure width is assumed to be identical for all slopes.

observation that there were no failures in the pine forest at Sedgwick Ranch, despite topographic characteristics similar to the sage and grassland hillslopes that failed.

A disequilibrium between root reinforcement and soil depths at Sedgwick Ranch is supported by field observations. First, there were nearly twice as many failures in the grass as in the sage, despite the generally lower hillslope gradients. This finding suggests that the grass slopes are currently more susceptible to failure. Second, failure depths, and therefore soil depths, were similar between the sage failures and the grass failures (Table 1), suggesting that soil depths in the grasslands may be relict features from a time when root reinforcement was higher. Finally, there were some failures on planar hillslopes in the grass (Fig. 2B), whereas all the failures in the sage were in hollows. Typically, shallow landslides occur in hollows owing to the long-term accumulation of sediment that results in thicker soils and the convergence of subsurface flow that leads to higher pore pressures (e.g., Hack and Goodlett, 1960; Dietrich and Dunne, 1978). Landslides on planar slopes, therefore, may again be an indication of soils that are too deep for the present root cohesion.

After this initial pulse of landsliding wanes, the frequency of landsliding will adjust to the new root conditions. The landsliding frequency should depend on the rate of hollow filling by both in situ soil production and soil transport into the hollow (Dietrich et al., 1995), root reinforcement, and the climate. If climate and the rate of hollow filling remain constant, landslide frequency on the converted hillslopes will remain elevated relative to that on the sage-covered hillslopes (Fig. 9). This difference can be explained simply in terms of mass conservation whereby the input of sediment into the hollows is balanced by the output from landsliding. Because the sediment storage within the hollows is limited by the root reinforcement and the grass roots can support only a thinner mantle of soil, the frequency of landsliding must increase to maintain the same sediment output.

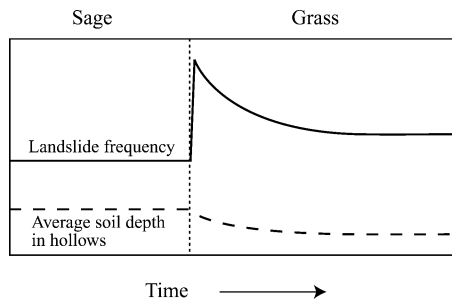


Figure 9. Transient and long-term effects of vegetation conversion from sage scrub to grass on soil depth in the bedrock hollows and the frequency of landsliding. The decline in root reinforcement triggers a pulse of landsliding throughout the landscape as the soils—which are initially thicker than grass can support—become more susceptible to failure. As soil depths in the grass-covered hollows reach a new equilibrium thickness, the frequency of landslides decreases from the peak rate but remains higher than in the sage-covered hollows if the rate of colluvium deepening remains constant under the change of vegetation.

CONCLUSIONS

The El Niño event of 1997–1998 brought record amounts of rainfall to the Santa Barbara region in California and triggered more than 150 shallow landslides at Sedgwick Ranch. The landslides were limited to coastal sage-scrub and converted grassland hillslopes, thus giving us the opportunity to study the mechanics of shallow landslides and to quantify the effects of vegetation conversion on sediment delivery to valley floors by landsliding. We present a slope-stability analysis that accounts for lateral-root reinforcement and accurately predicts an inverse relationship between hillslope angle and landslide volume in the sage. Field surveys indicate that volumes of failures in the grassland are not slope dependent and are generally smaller than those in the sage. To compare the sediment delivery from sage and converted grassland slopes, landscape-scale sediment fluxes were calculated for both. Although the spatial landslide frequency was higher in the grasslands, this factor was compensated by smaller volumes and shorter transport distances so that the failures on the sage hillslopes delivered more sediment to the valley floors. We suggest that the greater frequency of failures in the grasslands is due to a disequilibrium between soil depths and the ability of the grass roots to reinforce the soil. Over time, the soil in the grassland hollows will attain a shallower equilibrium depth.

ACKNOWLEDGMENTS

We thank J. Gabet and B. Newton for help with surveying and field observations and W. Dietrich for discussions. T. Biggs is thanked for reviewing an earlier draft of the manuscript. D. Montgomery and K. Schmidt are gratefully acknowledged for their helpful reviews. Supplies and salary for E. Gabet were supported by University of California Water Resources grant UCAL-W-917, a Sigma Xi grant, and a Mildred Mathias grant. Aerial photographs were paid for with funds from National Science Foundation grant SGER DEB9813669.

REFERENCES CITED

- Bailey, R.G., and Rice, R.M., 1969, Soil slippage: An indicator of slope instability on chaparral watersheds of southern California: *Professional Geographer*, v. 21, no. 3, p. 172–177.
- Campbell, R.H., 1975, Soil slips, debris flows, and rainstorms in the Santa Monica Mountains and vicinity, southern California: U.S. Geological Survey Professional Paper 851, 51 p.
- Corbett, E.S., and Rice, R.M., 1966, Soil slippage increased by brush conversion: Berkeley, California, U.S. Forest Service Pacific Southwest Forest and Range Experiment Station Research Note, PSW-128, p. 1–8.
- Craig, R.F., 1978, *Soil mechanics*: New York, Van Nostrand Reinhold Company Ltd., 318 p.
- Dibblee, T.W.J., 1993, Geologic map of the Figueroa Mountain Quadrangle: Santa Barbara, California, Dibblee Geological Foundation, scale 1:24,000.
- Dietrich, W.E., and Dunne, T., 1978, Sediment budget for a small catchment in mountainous terrain: *Zeitschrift für Geomorphologie*, suppl. band 29, p. 191–206.
- Dietrich, W.E., Reiss, R., Hsu, M.L., and Montgomery, D.R., 1995, A process-based model for colluvial soil depth and shallow landsliding using digital elevation data: *Hydrological Processes*, v. 9, p. 383–400.
- Hack, J.T., and Goodlett, J.C., 1960, Geomorphology and forest ecology of a mountain region in the Central Appalachians: U.S. Geological Survey Professional Paper 347, 66 p.
- Hamilton, J.G., 1997, Changing perceptions of pre-European grasslands in California: *Madrone*, v. 44, no. 4, p. 311–333.
- Hellmers, H., Horton, J.S., Juhren, G., and O'Keefe, J., 1955, Root systems of some chaparral plants in southern California: *Ecology*, v. 36, p. 667–678.
- Hibbert, A.R., 1971, Increases in streamflow after converting chaparral to grass: *Water Resources Research*, v. 7, p. 71–80.
- Kesseli, J.E., 1943, Disintegrating soil slips of the coast ranges of central California: *Journal of Geology*, v. 11, p. 342–352.
- Lustig, L.K., 1965, Sediment yield of the Castaic watershed, western Los Angeles County, California—A quantitative geomorphic approach: U.S. Geological Survey Professional Paper 422-F, 23 p.
- Montgomery, D.R., Schmidt, K.M., Greenberg, H.M., and Dietrich, W.E., 2000, Forest clearing and regional landsliding: *Geology*, v. 28, p. 311–314.
- Reistenberg, M.M., and Sovonick-Dunford, S., 1983, The role of woody vegetation in stabilizing slopes in the Cincinnati area, Ohio: *Geological Society of America Bulletin*, v. 94, p. 506–518.
- Reneau, S.L., and Dietrich, W.E., 1987, Size and location of colluvial landslides in a steep forested landscape, in Beschta, R.L., Blinn, T., Grant, C.E., Ice, G.G., and Swanson, F.J., eds., *Erosion and sedimentation in the Pacific Rim*: Wallingford, UK, International Association of Hydrological Sciences Press, p. 39–48.
- Reneau, S., Dietrich, W.E., Donahue, D.J., Hull, A.J., and Rubin, M., 1990, Late Quaternary history of colluvial deposition and erosion in hollows, central California coast ranges: *Geological Society of America Bulletin*, v. 102, p. 969–982.
- Rice, R.M., and Foggini, G.T.B., 1971, Effect of high intensity storms on soil slippage on mountainous watersheds in southern California: *Water Resources Research*, v. 7, p. 1485–1496.
- Rice, R.M., Corbett, E.S., and Bailey, R.G., 1969, Soil slips related to vegetation, topography, and soil in southern California: *Water Resources Research*, v. 5, p. 647–659.
- Scott, K.M., 1971, Origin and sedimentology of 1969 debris flows near Glendora, California: U.S. Geological Survey Professional Paper 750-C, 6 p.
- Selby, M.J., 1993, *Hillslope materials and processes*: Oxford, Oxford University Press, 451 p.
- Sidle, R.C., 1987, A dynamic model of slope stability in zero-order basins, in Beschta, R.L., Blinn, T., Grant, C.E., Ice, G.G., and Swanson, F.J., eds., *Erosion and sedimentation in the Pacific Rim*: Wallingford, UK, International Association of Hydrological Sciences Press, p. 101–110.
- Terwilliger, V.J., and Waldron, L.J., 1990, Assessing the contribution of roots to the strength of undisturbed, slip prone soils: *Catena*, v. 17, p. 151–162.
- Terwilliger, V.J., and Waldron, L.J., 1991, Effects of root reinforcement on soil-slip patterns in the Transverse Ranges of southern California: *Geological Society of America Bulletin*, v. 103, p. 775–785.
- Whipple, K.X., 1994, *Debris-flow fans: Process and form* [Ph.D. thesis]: Seattle, University of Washington, 205 p.

MANUSCRIPT RECEIVED BY THE SOCIETY SEPTEMBER 17, 2001

REVISED MANUSCRIPT RECEIVED FEBRUARY 4, 2002

MANUSCRIPT ACCEPTED MARCH 4, 2002

Printed in the USA